

OPTICAL CHARACTERISATION OF SEMI-TRANSPARENT PV MODULES FOR BUILDING INTEGRATION

Francisco-José Moralejo-Vázquez¹, Nuria Martín-Chivelet¹, Lorenzo Olivieri², Estefanía Caamaño-Martin²

¹ CIEMAT, Avda. Complutense, 40, 28040 Madrid (Spain).
franciscojose.moralejo@ciemat.es, nuria.martin@ciemat.es

² Instituto de Energía Solar – Technical University of Madrid, Avda. Complutense 30, 28040 Madrid (Spain).
lorenzo.olivieri@ies-def.upm.es, estefan@ies-def.upm.es

ABSTRACT: A complete characterisation of PV modules for building integration is needed in order to know their influence on the building's global energy balance. Specifically, certain characteristic parameters should be obtained for each different PV module suitable for building integrated photovoltaics (BIPV), some by direct or indirect measurements at the laboratory, and others by monitoring the element performance mounted in real operating conditions. In the case of transparent building envelopes it is particularly important to perform an optical and thermal characterization of the PV modules that would be integrated in them. This paper addresses the optical characterization of some commercial thin-film PV modules having different degrees of transparency, suitable for building integration in façades. The approach is based on the measurement of the spectral UV/Vis/NIR reflectance and transmittance of the different considered samples, both at normal incidence and as a function of the angle of incidence. With the obtained results, the total and zoned UV, visible and NIR transmission and reflection values are calculated, enabling the correct characterization of the PV modules integrated in façades and the subsequent evaluation of their impact over the electrical, thermal and lighting performance in a building.

Keywords: *a-Si*, BIPV, optical characterization, spectrophotometry

1 INTRODUCTION

The characterization of PV modules from the electrical, thermal and optical points of view is necessary to obtain an energy efficient building integration of photovoltaics (BIPV). According to the current European regulations about the energy performance of buildings and energy efficiency, such as Directives 2010/31/EU, and 2012/27/EU respectively [1], [2], the methodology should consider thermal characteristics, adequate natural lighting, heating and air-conditioning installations, application of energy from renewable sources, passive heating and cooling elements, shading, indoor air-quality, and design of the building.

Besides, the European norms about glass in building, such as EN 410:2011 [3] and EN 12898:2001 [4], specify some methods of determining the luminous and solar characteristics of glazing in buildings that serve as a base for lighting, heating and cooling calculations of rooms and permit the comparison between different types of glazing. These methods can be applied to a wide range of glazing systems, including PV modules designed to be integrated into the façade. Nevertheless, they don't include aspects such as the angle dependent properties of the laminates or the active behaviour of glazing (photovoltaic systems, electrochromic glass,...), something to consider for a more accurate knowledge of their real operating performance, as some authors have proved for PV modules working in PV power plants [5], [6].

In this work the authors have considered the main aspects that should be included in the optical characterisation of semi-transparent PV modules for building integration, as façade glass laminates. The measurements have been performed on different samples of amorphous silicon (*a-Si*) semi-transparent PV double glass laminates, having different transparency degrees.

Spectral reflectance and transmittance properties (R , T), in the ultraviolet, visible and near infrared (UV/Vis/NIR) ranges were measured.

The experimental results have allowed the characterization of the spectral performance of the PV laminates when reflecting or transmitting the radiation, at normal incidence and at other angles of interest. Moreover, with these measurements, weighted by different types of radiation source spectra and detector spectral responses, the luminous and thermo-radiative behavior of the PV laminated glasses have been characterized and analyzed.

2 TECHNICAL APPROACH

2.1 Experimental assembly

The considered samples were provided by Soliker[®] (Unisolar Group S.A.). They have been obtained from commercial BIPV laminate glasses, based on *a-Si* technology, *SOLGLASS e (3+3)* [7].



Figure 1: Some of the characterised PV modules and samples (Courtesy: Soliker[®]).

The samples have different nominal degrees of transparency: 0%, 10%, 20%, 30% and 40%. For comparison purposes, a sample without silicon has been also considered, having the same structure as the rest (see Figure 1). They'll be denoted respectively as $\{aSi0, aSi10, aSi20, aSi30, aSi40, aSi100\}$ in this report.

The PV modules architecture is as follows: Onto a 3.2 mm glass substrate coated with a transparent conductive oxide (TCO), AGC Solar AN10 [8], the a -Si/tandem a -Si solar cells have been deposited together with their back contacts. Then, the resulting structure is back encapsulated with a 0.45 mm EVA sheet and a 3.2 mm float glass, providing the PV laminated glass final product. The solar, luminous and electric basic characteristics included in the data sheets are shown below (see Table I).

Table I: Nominal characteristics of the modules (Data from Soliker[®] datasheets).

		$aSi0$	$aSi10$	$aSi20$	$aSi30$	$aSi40$
Laminated properties						
τ_v (%)	0,2%	0.2	10.8	17.3	28.4	36.6
ρ_v (act. face) (%)		7.6	8.3	7.6	8.2	8.3
ρ_v (inn. face) (%)		61.0	52.9	47.8	37.9	32.1
τ_{UV} (%)	0,0%	0.0	1.5	1.5	4.7	5.1
τ_e (%)	0,2%	0.2	9.4	15.0	24.3	31.7
ρ_e (%)	14,8%	14.8	13.9	11.1	12.4	11.6
g -value (%)	22,0%	22.0	29.0	34.0	41.0	46.0
U -value ($W \cdot m^{-2} \cdot K^{-1}$)		5.7	5.7	5.7	5.7	5.7
Electrical characteristics						
P_{MPP} (W) ($\pm 5\%$)	49 $\pm 5\%$	49.0	35.0	30.0	25.0	20.0
V_{OC} (V)	64,5	64.5	59.5	59.5	59.5	59.5
I_{SC} (A)	1,05	1.05	0.89	0.79	0.64	0.52

The measurements of the spectral UV/Vis/NIR reflectance and transmittance of the different samples considered have been done both at perpendicular incidence and as a function of the angle of incidence. In this second scenario, the objectives have been to derive conclusions about their angular behaviour and, based on that, to evaluate the derived properties of the glasses in orientations closer to those more common in buildings for these elements, especially in façade configurations. These angular dependence measurements have been done only in the PV active side (outer side). Summarizing, the tests could be categorised in:

- Hemispherical (H) and Diffuse (Df) Reflectance and Transmittance measurements at perpendicular angle of incidence of the radiation (denoted as HR, DfR, HT, and DfT),
- Directional (D) Reflectance and Transmittance measurements at different angles of incidence of the radiation (denoted as DR(##°), and DT(##°)).

The experiments have been done with a *Perkin Elmer[®] Lambda 900 UV/Vis/NIR spectrometer* equipped with a *LabSphere[®] 150 mm integrating sphere Spectralon[®]* coated [9], [10]. The integrating sphere provides a bigger effective collection surface to the detectors, equivalent to the sphere input ports area (1

in/25.4 mm). For the angle dependent directional R/T measurements, a *Directional Reflectance/Transmittance Set* [11], [12], [13], from *TNO Institute of Applied Physics*, has been used (see Figure 2). This accessory was developed by *TNO* for the *Perkin Elmer Lambda 800/900* and *Lambda 850/950/1050* types of spectrophotometers in the ADOPT project framework [14] and subsequently proved in the ALTSET project [15].



Figure 2: *Perkin Elmer[®] Lambda 900* equipped with *LabSphere[®] 150 mm integrating sphere* and the *TNO Directional R/T set*

The normal hemispheric and diffuse transmittance and reflectance measurements have been taken placing the samples on the entry and exit ports of the integrating sphere, respectively. The *Spectralon[®]* reflectance standards have been removed in the diffuse transmittance and reflectance measurements, in order to exclude the corresponding specular component of the transmitted or reflected radiation. In the current work, the UV/Vis/NIR wavelength range considered was 250 nm – 2500 nm.

2.2 Theoretical considerations

The methods of determining the luminous and solar characteristics of glazing in buildings based on spectral reflectance and transmittance measurements are detailed in the European Standard EN 410:2011 about glass in building [3], as mentioned in §1. Weighting calculations using R/T spectral measurements to obtain these characteristics are described in this standard. The need to consider the spectral (λ) reflectance and transmittance is due to the dispersive nature of the PV laminated glass' constituent materials. Besides the standard, in this study the angle of incidence (α) dependences of the spectral reflectance and transmittance have been considered, as they impact on these luminous and solar characteristics. Therefore, $R(\lambda, \alpha)$, $T(\lambda, \alpha)$ have been measured.

Spectral transmittance $T(\lambda, \alpha)$ is a critical property in the evaluation of the behavior and efficiency of any structural building glass. It allows the calculation of the quantity and quality of the optical radiation that passes through the glass and is useful for daylighting. The quantity of light is characterized by the Light Transmittance Factor, $\tau_v(\alpha)$, which represents the fraction of the incident light coming from a D65 standard illuminant with similar spectrum to daylight that passes through the glass and is viewed by a standard photopic observer:

$$\tau_v(\alpha) = \frac{\sum_{\lambda=380 \text{ nm}}^{780 \text{ nm}} D_{\lambda}^{D65} T(\lambda, \alpha) V(\lambda) \Delta\lambda}{\sum_{\lambda=380 \text{ nm}}^{780 \text{ nm}} D_{\lambda}^{D65} V(\lambda) \Delta\lambda} \quad [1]$$

where D_{λ}^{D65} is the relative spectral distribution of the standard illuminant D65 [17], and $V(\lambda)$ is the spectral luminous efficiency of the standard photopic observer [17].

The quality of the optical spectrum reproduction through the glass, that is, the accuracy in the colors reproduction, is characterized by the CIE General Color Rendering Index (CRI), R_a . Its explicit calculation is described in detail in reference [18].

On the other hand, spectral transmittance also allows to calculate the total direct solar radiation transmission through the glass. The Solar Direct Transmittance τ_e is the required parameter for characterizing this concept. It represents the fraction of the incident solar radiation that passes through the glass:

$$\tau_e(\alpha) = \frac{\sum_{\lambda=300 \text{ nm}}^{2500 \text{ nm}} S_{\lambda} T(\lambda, \alpha) \Delta\lambda}{\sum_{\lambda=300 \text{ nm}}^{2500 \text{ nm}} S_{\lambda} \Delta\lambda} \quad [2]$$

where S_{λ} stands for the standard *AM1.0G* relative spectral distribution of solar radiation for a 1.0 air mass and some other established conditions, (see reference [19]).

Spectral reflectance $R(\lambda, \alpha)$ is also an important property in the evaluation of the behavior of any building structural glass. The front side spectral reflectance together with the transmittance, allows the calculation of other characteristic parameters, such as the Total Solar Energy Transmittance, also named as (center-of-glass) Solar Heat Gain Coefficient (SHGC), Solar Factor, g -value or simply g , see reference [3]. This parameter represents the total solar energy transmitted indoors by the fenestration, both by direct transmission and by the indoor emission of part of the absorbed energy:

$$g(\alpha) = \tau_e(\alpha) + q_i(\alpha) \rightarrow q_i(\alpha) = \alpha_e(\alpha) \cdot \frac{h_i}{h_i + h_e} \quad [3]$$

$\alpha_e(\alpha) = 1 - \tau_e(\alpha) - \rho_e(\alpha)$; with

$$\rho_e(\alpha) = \frac{\sum_{\lambda=300 \text{ nm}}^{2500 \text{ nm}} S_{\lambda} R(\lambda, \alpha) \Delta\lambda}{\sum_{\lambda=300 \text{ nm}}^{2500 \text{ nm}} S_{\lambda} \Delta\lambda}.$$

where q_i is the secondary internal heat transfer factor, α_e is the Solar Absorptance Factor, ρ_e is the Solar Reflectance Factor, , and h_i, h_e are the internal and the external heat transfer coefficients of the sample surfaces,

respectively.

The rear side spectral reflectance, in the particular case of PV laminated glasses, is also an important parameter which is related not only with the aesthetic appearance of the glass from inside, but also may affect significantly the indoor illumination. Some metallic back contacts of the solar cells could have a strong impact on the illumination of the room, as they show high reflectance values. The Luminous Reflectance is the parameter that characterizes this effect. This parameter is defined as the fraction of the incident light from a reference illuminant that is reflected and viewed by a standard photopic observer. As reference illuminants D65 and F2 standard illuminants have been considered. The first one stands for daylight and the second one for a conventional workplaces fluorescent lamp, in order to consider both natural and artificial illumination:

$$\rho_v^{Rear}(D65) = \frac{\sum_{\lambda=380 \text{ nm}}^{780 \text{ nm}} D_{\lambda}^{D65} R(\lambda) V(\lambda) \Delta\lambda}{\sum_{\lambda=380 \text{ nm}}^{780 \text{ nm}} D_{\lambda}^{D65} V(\lambda) \Delta\lambda} \quad [4]$$

$$\rho_v^{Rear}(F2) = \frac{\sum_{\lambda=380 \text{ nm}}^{780 \text{ nm}} D_{\lambda}^{F2} R(\lambda) V(\lambda) \Delta\lambda}{\sum_{\lambda=380 \text{ nm}}^{780 \text{ nm}} D_{\lambda}^{F2} V(\lambda) \Delta\lambda}$$

where D_{λ}^{D65} , D_{λ}^{F2} are the relative spectral distributions of the standard illuminants D65 and F2 respectively [17].

Other considered parameters from the standard EN 410:2011 on glass in building [3] are the Shading Coefficient SC , directly related to g -value, which represents the comparison between the g -value of the tested glass and of 3 mm clear float glass, and the Ultraviolet Transmittance of the glass τ_{UV} , concerning the radiation damage to the different materials in the room, i.e. commercial goods,...

$$SC(\alpha) = \frac{g(\alpha)}{0.87}; \quad [5]$$

$$\tau_{UV} = \frac{\sum_{\lambda=280 \text{ nm}}^{380 \text{ nm}} U_{\lambda} T(\lambda) \Delta\lambda}{\sum_{\lambda=280 \text{ nm}}^{380 \text{ nm}} U_{\lambda} \Delta\lambda} \quad [6]$$

where U_{λ} represents the relative spectral distribution of standard solar UV radiation.

Finally, the Selectivity Index S was considered to compare light and thermal performance of the PV laminates [20]. This index is used to evaluate the degree of light transmissivity versus the degree of total energy transmittance, and it is a good indicator of the glass capacity to transmit daylight without extra thermal charge:

$$S(\alpha) = \frac{\tau_v(\alpha)}{g(\alpha)} \quad [7]$$

This parameter is not included in the EN 410:2011 standard, but it is widely considered by the glass industry.

3 RESULTS

3.1 Transmittance measurements

The hemispheric transmittance spectral distributions at normal incidence are shown in Figure 3. It is observed the UV and NIR (from 1750 nm onwards) wavelengths filtering capacity of all the samples. Two different trends can be distinguished in the visible range: a rapid growth from 380 nm to 550 nm, and a smooth dependence with the wavelength from 550 nm to 800 nm, having a maximum transmittance value near 650 nm. In the NIR the general tendency is to decrease with the wavelength up to 2500 nm where all the transmittances become nearly zero. It is also important to highlight that the detected signal above the 2250 nm is noisy because of the weak incoming signal and the limited NIR detection capability of system in this range. In order to associate each different sample with a more accurate transparency value than the nominal one, the integral of these transmittance spectral distributions has been used in each case. It will be the abscissa in all the graphs representing any property versus transparency.

The results show the influence of the transparency in the loss of usable radiation for the PV conversion, as the transmission curves match with the amorphous silicon spectral response (*a-Si* – SR) typical distribution, in a big extent (~ 320 nm to ~ 800 nm). The amount of losses depends on the transparency but also on the angle of incidence, as shows Figure 4. On the other side, the transmission curves show the possibilities of modulating the passive control of daylight and incoming energy into the building.

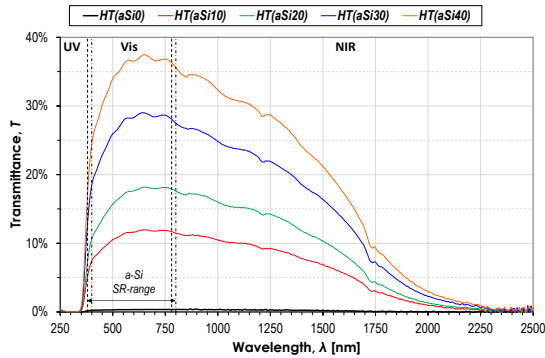


Figure 3: Spectral hemispheric transmittance of the samples at normal incidence

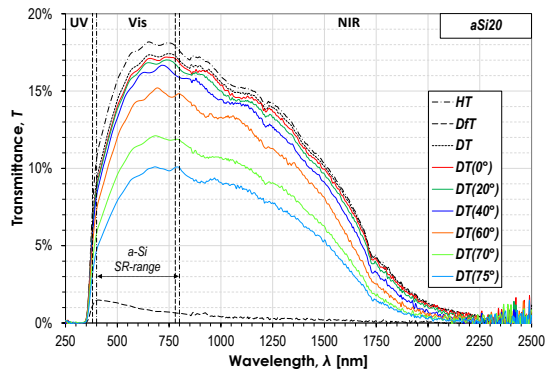


Figure 4: Spectral directional transmittance of *aSi20* sample, for the different angles considered, together with the total hemispheric and diffuse transmittances.

The diffuse transmittance spectrum obtained in all cases mainly concerns the optical wavelengths, e.g. for *aSi20* sample see Figure 4. In this case it varies between 0.7% and 1.5% and reaches a maximum of 12.5% of the hemispheric value around 400 nm.

3.2 Reflectance measurements

The hemispheric reflectance spectral distributions of the PV active side of the laminates are shown in Figure 5. The curves exhibit three different regions: In the first one, at optical wavelengths up to 650 nm, the curves show a very similar reflectance behavior in all the samples, independently of the transparency, having low values that vary from 5% to 10% as a function of the wavelength. This behavior is favorable to the PV conversion, as this low reflectance range matches the *a-Si* spectral response to a great extent.

In the second region, from 700 nm to 1850 nm, the shapes oscillate without a common pattern but all show an absolute maximum between 1000 nm and 1250 nm. Finally, in the last part of the spectra, from 1850 nm on, all the samples present a quasi-linear increase of the reflectance with the wavelength. They have a small level of noise added, as in the case of the transmittance (2250 nm – 2500 nm).

Besides, Figure 6 shows the angle dependence of the spectral reflectance of one of the samples. In all cases the reflectance curves move to higher values as the angle of incidence increases. This behavior originates PV conversion losses, as can be deduced from the figure. Single reflectance values up to 25.0% were measured for *aSi20* sample at 70° angle of incidence, which is a common operating condition in structural building glasses in façades and medium latitudes.

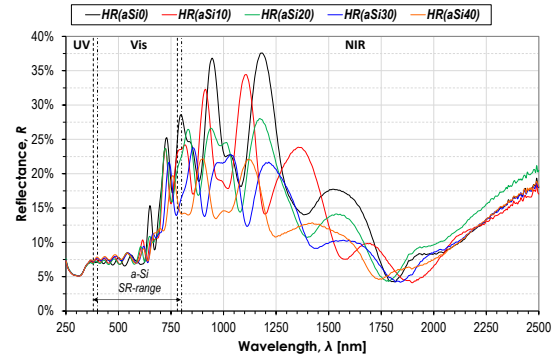


Figure 5: Spectral hemispheric reflectance of the samples at normal incidence

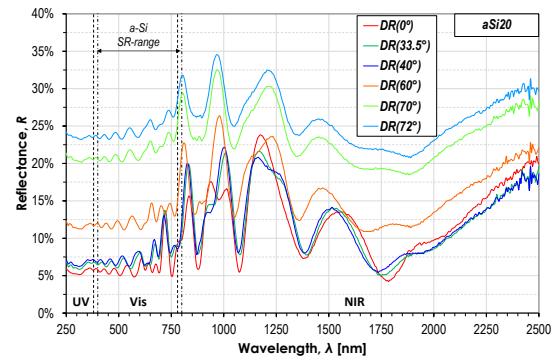


Figure 6: Spectral directional reflectance of *aSi20* sample, for the different angles considered

The diffuse reflectance spectra obtained, as shown in Figure 7 for the *aSi20* sample, exhibits a smooth increase with the wavelength in the UV/Vis region up to 650 nm. From this point to the Vis/NIR border, it increases up to a maximum and then, decreases reaching zero at 1750 nm. For the *aSi20* sample, the maximum of 12.3% at 815 nm represents 50% of the hemispheric reflectance at this wavelength, whereas in the *a-Si* spectral response region, the diffuse reflectance ranged between 20% - 25% approximately.

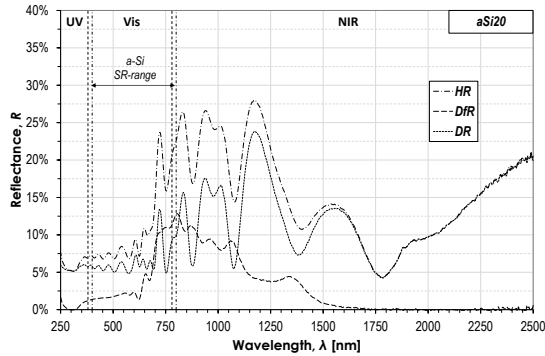


Figure 7: Spectral hemispheric, diffuse and specular reflectance of *aSi20* sample at normal incidence

On the other hand, the non-active hemispheric reflectance spectral distributions of the laminates are shown in Figure 8. These distributions have a hump in the optical wavelengths with a maximum value in this range obtained around 600 nm. From 800 nm on there is a general continuous increase up to 1650 nm in the NIR, with a dependence that decreases with the transparency. They exhibit a minimum in 1730 nm and have another quasi-plate zone between this minimum and another one in 2300 nm. These shapes are common in soda-lime-silica float glasses, as it is the rear glass of these laminates.

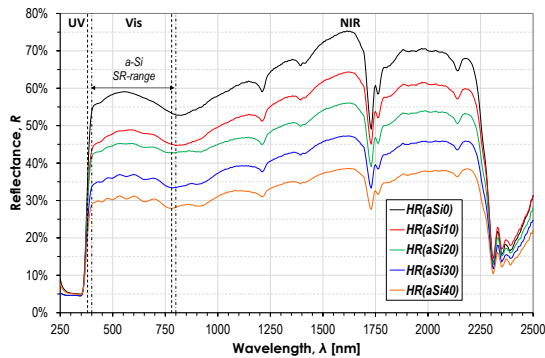


Figure 8: Spectral hemispheric reflectance of the backside of samples at normal incidence

All the measured back-reflectances show high diffuse components, which cause a high impact on the hemispherical one, especially in optical wavelengths and up to 1650 nm (see Figure 9, for the *aSi20*). The curves have a maximum at 400 nm and progressively decrease along the considered range. The percentage of diffuse back reflectance varies from 80% to 14% of the hemispheric reflectance measured.

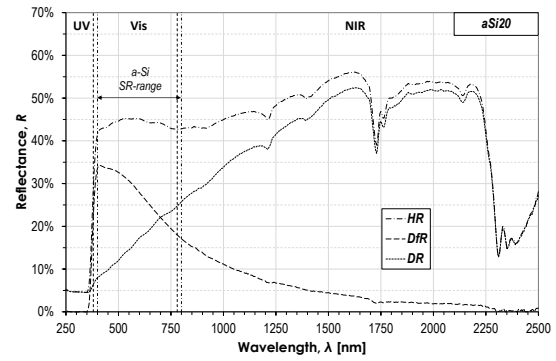


Figure 9: Spectral hemispheric, diffuse and specular reflectances of the *aSi20* sample backside at normal incidence

3.3 Luminous characteristics of the PV glazing

The luminous transmittance of these PV laminated glasses rises linearly with the integrated UV/Vis/NIR transmittance (see Figure 10). Besides, it decreases with the angle of incidence, an average percentage of 32.4% from 0° to 70°, with small deviations depending on the PV module considered (see results on Table II). In this case, the decrease is not linear: Light transmittance decreases more sharply from 60 degrees on (see Figure 11).

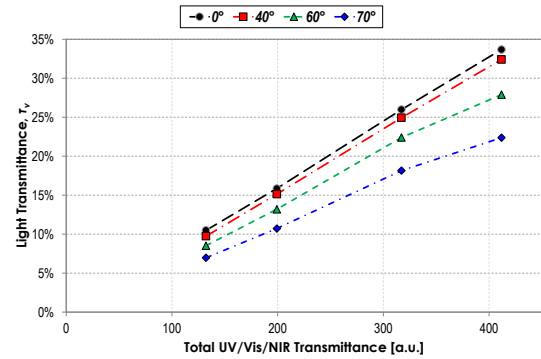


Figure 10: Light Transmittance vs. Integrated Transmittance, for the different angles considered.

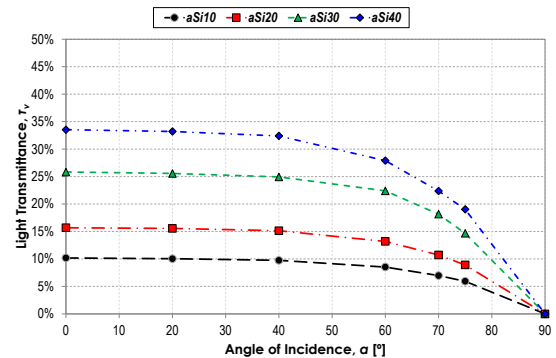
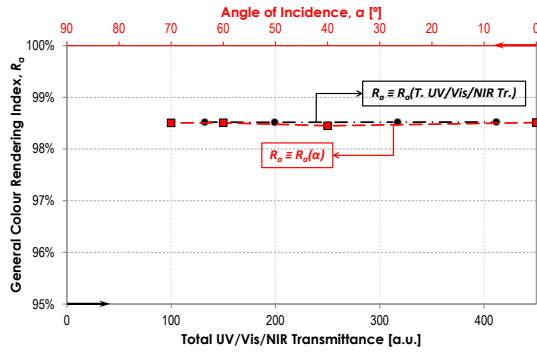


Figure 11: Light Transmittance dependence with the angle of incidence, for each different sample.

Table II: Light Transmittance Results, τ_v (%)

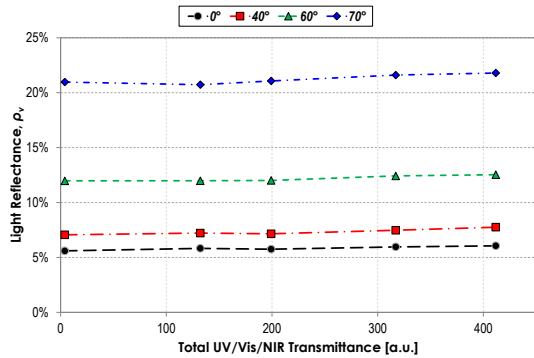
	0°	40°	60°	70°
Sample				
<i>aSi10</i>	10.5	9.8	8.5	7.0
<i>aSi20</i>	15.9	15.1	13.2	10.7
<i>aSi30</i>	26.0	24.9	22.4	18.2
<i>aSi40</i>	33.7	32.4	27.9	22.4

Regarding the color rendering index, R_a it is practically constant with the transparency and the angle of incidence. All the samples show high rendering indexes, around 98.5% (see Figure 12).

**Figure 12:** General Color Rendering Index vs. Integrated Transmittance, for each different sample and the angles of incidence considered.

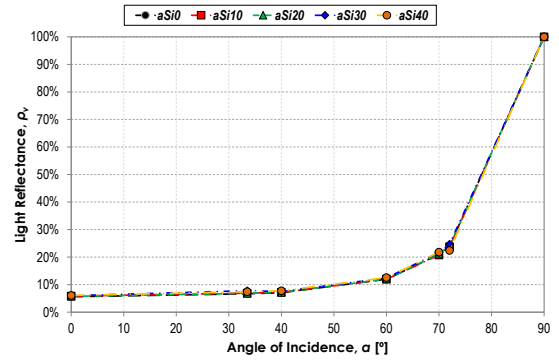
This results are quite similar to those of conventional building glasses and, sometimes, improve the values in solar control glasses (e.g. Interpane® ipascreen E [20] with $R_a = 97\%$), ensuring an accurate color perception of the objects in the room.

On the other side, the active side light reflectance depends slightly on the integrated transmittance in the UV/Vis/NIR range (see Figure 13). Its value increases with the incident angle from an average value of 5.8% at normal incidence to 21.2% at 70° , varying slightly depending on the PV module considered (see the specific results on Table III).

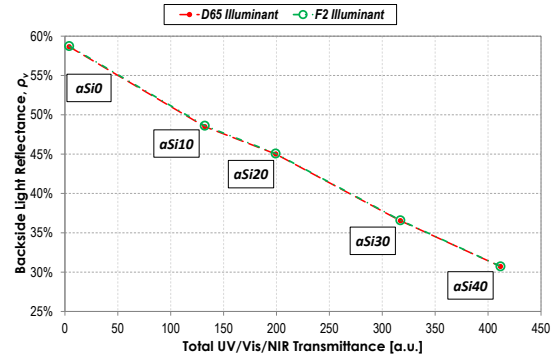
**Figure 13:** Light Reflectance vs. Integrated Transmittance, for the different angles considered**Table III:** Light Reflectance, ρ_v (%)

	0°	40°	60°	70°
Sample				
<i>aSi0</i>	5.6	7.1	12.0	21.0
<i>aSi10</i>	5.8	7.2	12.0	20.7
<i>aSi20</i>	5.8	7.2	12.0	21.1
<i>aSi30</i>	6.0	7.5	12.4	21.6
<i>aSi40</i>	6.1	7.8	12.5	21.8

The light reflectance angle dependence is similar for all samples and follows a quasi-exponential type increase (see Figure 14). Results show that this dependence is determined by the frontal glass, regardless of how much transparent the samples are.

**Figure 14:** Luminous Reflectance evolution with the angle of incidence, for each different sample.

In contrast, the backside light reflectance of the samples varies significantly with the integrated transmittance in the UV/Vis/NIR range (Figure 15), falling quasi-linearly from 58.7% (*aSi0*) to 30.7% (*aSi40*) at perpendicular incidence.

**Figure 15:** Luminous Reflectance vs. Integrated Transmittance, for the backside of the different samples

3.4 Solar characteristics of the PV glazing

The solar energy transmission, characterized by the Solar Factor (g -value), varies linearly between 0.22 and 0.44 for the different integrated transmittance values at perpendicular incidence (see Figure 16). It's observed that the bigger the considered angle of incidence, the weaker the linear dependence.

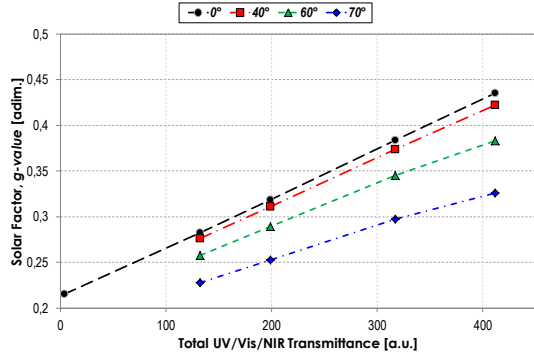


Figure 16: Solar Factor Solar vs. Integrated Transmittance, for the different angles considered

This angle dependence of the solar factor is shown in Figure 17, which also includes the angle of incidence performance of a *SGG STADIP SILENCE 55.1* [21] conventional laminate, for comparison. The values are included in Table VI. Some differences with the conventional laminate can be seen regarding the two terms of g -value.

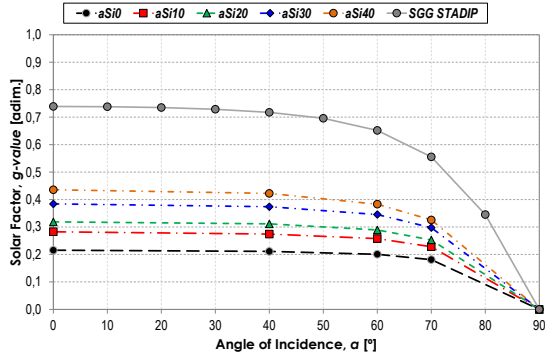


Figure 17: Solar Factor dependence with the angle of incidence, for each different sample.

The laminates under study have lower solar direct transmittance and higher secondary internal heat transfer factor than common glazing elements (see Table IV and Table V). A low Solar Direct Transmittance implies low percentage of solar radiation transmitted. As Solar Reflectance is also low, the absorption in the laminate is very high, and this energy is reemitted as heat, as the PV laminates do not generate electricity, in this case. Considering the poor thermal isolation of laminates, it supposes a high internal heat transmission. The use of real operating PV modules would partially reduce this heat considering the amount of incident energy converted into electrical power output. However, both components are balanced resulting in g -values (Table VI) and selectivities (Table VII) that are compatible with passive solar control systems

Table IV: Solar Direct Transmittance Results, τ_e (%)

	0°	40°	60°	70°
Sample				
<i>aSi10</i>	9.0	8.4	7.3	6.0
<i>aSi20</i>	13.7	13.1	11.5	9.3
<i>aSi30</i>	22.1	21.2	18.8	15.2
<i>aSi40</i>	28.7	27.4	23.6	18.8
<i>SGG STADIP*</i>	68.0	65.4	58.4	48.8

Table V: Secondary Internal Heat Transfer Factor, q_i (%)

	0°	40°	60°	70°
Sample				
<i>aSi10</i>	19.4	19.2	18.4	16.8
<i>aSi20</i>	18.2	18.1	17.4	16.0
<i>aSi30</i>	16.3	16.2	15.7	14.6
<i>aSi40</i>	14.9	14.8	14.7	13.8
<i>SGG STADIP*</i>	5.9	6.4	6.8	6.7

Table VI: Solar Factor Results, g -value

	0°	40°	60°	70°
Sample				
<i>aSi10</i>	0.28	0.28	0.26	0.23
<i>aSi20</i>	0.32	0.31	0.29	0.25
<i>aSi30</i>	0.38	0.37	0.35	0.30
<i>aSi40</i>	0.50	0.48	0.44	0.37
<i>SGG STADIP*</i>	0.74	0.72	0.65	0.56

(*Source: Prepared by the authors on the basis of data supplied by CIEMAT-DER/UiE3 [22])

On the other side, Figure 18 shows the UV transmittance of the samples. The two most transparent ones (*aSi30* and *aSi40*) are slightly higher than the one of a clear conventional laminated glass *SGG STADIP SILENCE 55.1* [21] ($\tau_{uv} = 2\%$). This could mean a limitation in the potential applications of this kind of elements as façade glazing. Nevertheless, this UV transmittance is not different to that of the advanced solar control glazing, such as *SGG COOL-LITE ST150* [21] with values up to $\tau_{uv} = 21\%$ depending on the multilayer configuration.

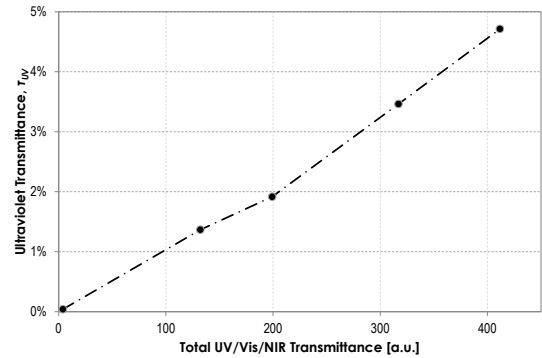


Figure 18: UV Transmittance vs. Integrated Transmittance of the different samples

Finally the selectivity of the samples has been calculated (see Table VII). For comparison purposes, some commercial glasses with different characteristics (from simple glazing to active solar control glazing) have been included also in the table. It is important to highlight that active glazing can reach selectivity values up to 4 or 5. As can be seen in Table VII, the selectivity of the laminates under study is lower than those of commercial glazing. These lower values are due to the limited capacity of daylight transmission.

Table VII: Selectivity Results, S

	0°	40°	60°	70°
Sample				
<i>aSi10</i>	0.37	0.35	0.33	0.31
<i>aSi20</i>	0.50	0.49	0.46	0.42
<i>aSi30</i>	0.68	0.67	0.65	0.61
<i>aSi40</i>	0.77	0.77	0.73	0.69
<i>SGG STADIP Silence</i>	1.16	---	---	---
<i>SGG COOL-LITE ST</i>	1.00	---	---	---
<i>INTERPANEScreenE</i>	1.29	---	---	---

4 CONCLUSIONS

A measurement campaign has been carried out with the goal of optically characterizing a set of semi-transparent PV laminated glasses, based on thin film amorphous silicon technology (*a-Si*), and suitable for building integration as multi-functional structural glasses. The EN 410:2011 and EN 12898:2011 European standard protocols to determine the luminous and the solar characteristics of glass in building [3], [4], based on the measurement of spectral reflectance and transmittance UV/Vis/NIR, have been considered. In addition, the influence of the angle of incidence on these characteristic parameters has been also measured and analyzed. Table VIII lists the main results of the standard parameters obtained for each considered sample.

Summarizing, there are two fundamental variables in this study, namely, the transparency degree and the angle of incidence of radiation, in the assessment of the performance of these PV laminated glasses as multifunctional building elements.

The shapes of transmittance and reflectance spectral profiles indicate that the laminate glasses considered have been optimized to be used as PV modules. Nevertheless, the final results of this work indicate also that their good properties in terms of daylighting and solar control

capabilities allow a possible efficient integration in glazing façades. From the luminous point of view, regarding the inside of the building, the devices are compatible with standard glazing and with complex solar control glazing, improving the rendering colors quality of the last ones. The greatest problem with them could be the glare due to the high internal reflectance, especially of those more opaque. Outwards, the low reflectance in the visible range avoids the potential glare problems in the outside of the building.

In the thermo-radiative aspects, the performance of these laminates is equivalent to that of the most common solar control glazing. It is important to highlight that the distribution among direct transmission of energy and secondary transfer is quite different, but achieves the same global behavior.

It is very important to emphasize that, in this work, the active performance of the PV laminate glasses from Soliker® hasn't been considered. This may have disadvantaged them in comparison with commercial advance active systems of glazing for solar control, e.g. electrochromic glazing with thermal insulation [20], which has better luminous and solar characteristics. Further steps in this research on BIPV semi-transparent building elements will contemplate the variability of the optical characteristics on the basis of the operating point and will consider, among other aspects, the active performance of PV modules.

According to the results obtained, it should be also noted the importance of considering the angular dependence of the properties in order to obtain more accurate and realistic evaluations of the solar systems performance. In this sense, efforts were done in order to assess the real net losses of radiation useful for PV conversion and daylight and the real net gains of solar energy indoor, in specific locations and orientations, depending on the season.

Table VIII: Luminous and solar properties obtained according to EN 410:2011 and calculated Selectivity.

		<i>aSi0</i>	<i>aSi10</i>	<i>aSi20</i>	<i>aSi30</i>	<i>aSi40</i>
Property						
Light Transmittance	τ_v	---	11.2%	17.0%	27.5%	35.7%
Light Reflectance (act. face)	ρ_v^{D65}	7.5%	7.9%	7.8%	7.9%	7.9%
Light Reflectance (inn. face)	ρ_v^{D65}	58.7%	48.5%	45.0%	36.5%	30.7%
Light Reflectance (inn face)	ρ_v^{F2}	58.7%	48.6%	45.1%	36.6%	30.7%
Solar Direct Transmittance	τ_e	0.3%	9.6%	14.5%	23.2%	30.1%
Solar Direct Reflectance (act. face)	ρ_e	15.1%	13.7%	13.7%	12.5%	11.3%
Solar Direct Absorptance (act. face)	α_e	84.6%	76.8%	71.9%	64.4%	58.6%
g-value	g	0.20	0.28	0.31	0.38	0.44
Shading Coefficient	SC	0.23	0.32	0.36	0.44	0.50
Ultraviolet Transmittance	τ_{UV}	0.0%	1.4%	1.9%	3.5%	4.7%
General Color Rendering Index	R_a	---	98.5%	98.5%	98.5%	98.5%
Selectivity*	S	---	0.40	0.54	0.72	0.81

5 ACKNOWLEDGMENTS

The authors are grateful to Soliker (Unisolar Group S.A.) for their support and for the supply of samples. The authors also thank José-Lorenzo Balenzategui and Ricardo Enriquez (CIEMAT-DER, Madrid) for their valuable help to carry out this work.

6 NOMENCLATURE

Terminology

a-Si = amorphous silicon
aSi0 = Soliker SOLGLASS e opaque
aSi10 = Soliker SOLGLASS e 10% Transp.
aSi20 = Soliker SOLGLASS e 20% Transp.
aSi30 = Soliker SOLGLASS e 30% Transp.
aSi40 = Soliker SOLGLASS e 40% Transp.
aSi100 = Soliker SOLGLASS e without *a-Si* cells

Nomenclature

HT = Normal Hemispherical Transmittance
DfT = Normal Diffuse Transmittance
DT = Normal Directional Transmittance
DT(##°) = Directional Transmittance at ##°
HR = Normal Hemispherical Reflectance
DfR = Normal Diffuse Reflectance
DR = Normal Directional Reflectance
DR(##°) = Directional Reflectance at ##°
 α = Angle of Incidence
 τ_v = Light Transmittance
 ρ_v = Light Reflectance (act. face)
 ρ_v^{Rear} = Light Reflectance (inn face)
 $D_{\lambda}^{##}$ = Relative Spectral Distribution of ## Standard

Illuminant

D65 = CIE Standard Illuminant D65 (Daylight)
F2 = CIE Standard Illuminant F2 (Fluorescent lamp)
V(λ) = spectral luminous efficiency of the standard

photopic observer

τ_e = Solar Direct Transmittance
 ρ_e = Solar Direct Reflectance (act. face)
 α_e = Solar Direct Absorptance (act. face)
 S_{λ} = Relative Spectral Distribution of Standard Solar

Radiation AM 1.0G

AM 1.0G = Global standard spectra for 1.0 air mass
g = g-value
SC = Shading Coefficient
 τ_{UV} = Ultraviolet Transmittance
 U_{λ} = Relative Spectral Distribution of Standard *UV*

Solar Radiation

R_a = General Color Rendering Index
S = Selectivity

7 REFERENCES

- [1] Directive 2010/31/EU of the European Parliament and of the Council of 19 May 2010 on the energy performance of buildings
- [2] Directive 2012/27/EU of the European Parliament and of the Council of 25 October 2012 on energy efficiency
- [3] EN 410:2011 Glass in building - Determination of luminous and solar characteristics of glazing
- [4] EN 12898:2001 Glass in building – Determination of

the emissivity

- [5] N. Martín, J.M. Ruiz, Solar Energy Materials and Solar Cells 70 (2001) 25

- [6] J.P. Silva, G. Nofuentes, J.V. Muñoz, Journal of Solar energy Engineering 132 (2010) 041016/1

- [7] Soliker (Grupo Unisolar S.A.)
www.soliker.com/inicio-home.html

- [8] AGC Solar
<http://www.agc-solar.com/home.html>

- [9] PerkinElmer, Inc. Brochure on “High performance Lambda spectroscopy accessories”

- [10] PerkinElmer, Inc. Application Note UV/Vis/NIR on “Application and use of integrating spheres with the LAMBDA 650 and 850 UV/Vis and LAMBDA 950 UV/Vis/NIR spectrophotometers”

- [11] J.L. Taylor, PerkinElmer, Inc. Technical Note UV/Vis/NIR on “Reflectance measurements of materials used in the solar industry”

- [12] J. Sellors, P.A. van Nijnatten, P. Sanotra, Proceedings of the 7th International Conference on Coatings on Glass and Plastic (ICCG7) (2008)

- [13] P.A. van Nijnatten, Solar Energy 73 (3) (2002) 137

- [14] P.A. van Nijnatten, Proceedings of the World Renewable Energy Congress VI (WREC2000) (2000) 171

- [15] A. Maccari, P. Polato, Rivista della Staz. Sper. Del Vetro, 5 (2000)

- [16] W.J. Platzer, Proceedings of the 3rd International ISES Europe Solar Congress (EUROSUN 2000) (2000)

- [17] CIE 015:2004 Colorimetry, 3rd Edition

- [18] CIE 013.3:1995 Method of measuring and specifying colour rendering properties of light sources

- [19] CIE 085:1989 Solar spectral irradiance

- [20] “Interpane: Design with glass”, 8th Edition (2011)
http://www.interpane.com/design_with_glass_64.html

- [21] Saint Gobain Glass
<http://saint-gobain-glass.com/>

- [22] CIEMAT-DER/UiE3 and CIEMAT-PSA/LECE
<http://www.ciemat.es/cargarSubLineaInvestigacion.do?idEntificador=7&idArea=1&idLinea=6>, and
<http://www.psa.es/webeng/instalaciones/lece.php#lece>